Photoelectrochemical biosensor for detection of adenosine triphosphate in the extracts of cancer cells†

Xiaoru Zhang, Yanqing Zhao, Shuguo Li and Shusheng Zhang*

Received 1st September 2010, Accepted 8th October 2010
DOI: 10.1039/c0cc03595e

A photoelectrochemical sensing strategy for highly sensitive detection of small molecules was developed based on the recognition interaction between aptamer and target molecule—ATP.

The development of biosensors has become increasingly important in molecular diagnostics. Efforts have been made constantly to develop new methods with the goal to get higher sensitivity, lower cost and better reproducibility. Fluorescence,[1] chemiluminescence (CL)[2] and electrochemiluminescence (ECL)[3] are widely used in clinical diagnostic laboratories due to their high sensitivity. However, these methods employ optical detection, and the high instrument cost is a major disadvantage. Compared to optical detection methods, electrochemistry instrumentation is much simpler and lower cost. Among the various electrochemistry-based biosensors developed so far, the photoelectrochemistry approach has attracted a great deal of attention.[4] Due to the different forms of energy for excitation (light) and detection (current), this method is very sensitive with low background signals.[5] Although possessing remarkable advantages, photoelectrochemistry is mainly used in the field of solar cells. So far, the photoelectrochemical method has been used in the detection of DNA damage,[5] DNA,[4c,6] proteins[7] and small molecules.[8] However, compared to other analytical methods, the exploration of photoelectrochemical biosensors is limited and so it is desirable to improve the utilization of photoelectrochemistry in the area of analytical detection.

Known as the 'energy currency of life', ATP is the major energy source within the cell to drive a number of biological processes. In addition, ATP is a marker for cell viability because it is present in all metabolically active cells and its concentration declines very rapidly when the cells undergo necrosis or apoptosis.[9] Therefore, ATP monitoring can be used to assess the cytocidal, cytostatic and proliferative effects of a wide range of drugs, biological response modifiers, and biological compounds.[10]

Since DNA aptamer for ATP was first selected by Huizenga and Szostak in 1995,[11] there have been considerable efforts to develop aptasensors for ATP detection based on fluorescent,[12] electrochemical,[13] colorimetric,[14] CL[15] and ECL[16] methods. While each strategy has distinct advantages, each also presents its own unique set of limitations, such as poor sensitivity and high equipment cost. To the best of our knowledge, there are no photoelectrochemistry sensors for ATP detection. Due to the advantages inherent to photoelectrochemistry, such as high sensitivity and low instrument cost, here, we developed a photoelectrochemical aptasensor for the detection of ATP. By integrating the magnetic separation of magnetic beads (MB) and high sensitivity of the bio-barcode technique used in conventional analytical strategy,[17] ATP can be detected sensitively. At the same time, the application scope as well as detection methods of photoelectrochemical biosensors can be expanded accordingly.

The fabrication of the sensor is shown in Scheme 1. The bio-barcode was prepared by self-assembling of barcode DNA and binding DNA on AuNPs. Then the prepared bio-barcodes were conjugated to the aptamer modified MBs through hybridization. When target molecule ATP was introduced, because an aptamer can bind tightly and specifically to its target molecules with a binding constant greater than that of an ordinary double-stranded DNA,[13b] the double helixes were opened and the bio-barcodes were released into the solution. At the same time, an SnO_2 nanoparticle-modified ITO electrode was silanized with 3-aminopropyltriethoxysilane (APS) and then reacted with the cross-linking reagent glutaraldehyde by Schiff-base formation while the remaining aldehyde groups could be used to immobilize amine-capped aptamers. Then, the released bio-barcodes were captured by the aptamers assembled on the ITO electrode through hybridization. To form more dsDNA, complementary DNA was added, and then the introduced photoelectrochemically active species $Ru(bpy)_2dppz^{2+}$ could intercalate into the double helix of dsDNA. After illumination of the modified ITO electrode, the generated photocurrents were measured in the presence of electron donor sodium oxalate. Since more ATP molecules can release more bio-barcodes from MBs, which can be captured by the ITO electrode, consequently,

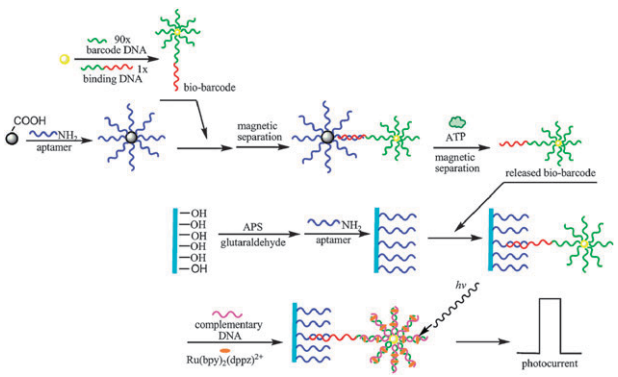

Scheme 1 Schematic diagram for the fabrication of the ATP biosensor and photoelectrochemical detection based on bio-barcode amplification.

State Key Laboratory Base of Eco-chemical Engineering, College of Chemistry and Molecular Engineering, Qingdao University of Science and Technology, Qingdao 266042, P. R. China.
E-mail: shushzhang@126.com; Fax: (+86) 532-84022750;
Tel: (+86) 532-84022750

† Electronic supplementary information (ESI) available: Experimental details and additional figures. See DOI: 10.1039/c0cc03595e

more photoelectrochemically active species $Ru(bpy)_2dppz^{2+}$ can be introduced, and higher photocurrent can be obtained. The developed photoelectrochemical biosensor can thus be used to detect ATP.

The prepared AuNPs have an average diameter of approximately 20 nm as measured by TEM (Fig. 1A). From the TEM of MB-bio-barcode conjugates shown in Fig. 1B, numerous AuNPs could be seen on the surface of the MB compared to the TEM of MB shown in Fig. 1C. The result showed that the MB-bio-barcode conjugates were prepared as expected.

Electrochemical impedance spectroscopy (EIS) is a powerful electro-analytical technique to probe the electron transfer kinetics of modified electrodes. As shown in Fig. 2, for a bare ITO electrode surface, the impedance spectrum exhibited a small semicircle (curve a). After adsorption of SnO_2 (curve b) and reacting with APS (curve c), R_{et} increased progressively. This increase in diameter indicated that the charge-transfer rate of $Fe(CN_6)^{3-/4-}$ was reduced gradually. When the electrode was assembled with aptamer DNA (curve d) and bio-barcode (curve e), the diameter of semicircular part greatly increased, suggesting the electron transfer of the redox-probe was obstructed by the assembled DNA strands, which slowed down the redox reaction of $Fe(CN_6)^{3-/4-}$. It was thus verified that the assembly process was successful.

Due to their specific characteristics of large surface area, high surface adsorption, good stability and high photo-to-electrical conversion efficiency, semi-conducting materials have been widely used in the field of dye-sensitized photochemical solar cells.[18] In order to enhance the quantity of semi-conductive material on electrode further, some work has been focused on spreading colloidal SnO_2[5] or TiO_2[19] on the surface of an indium tin oxide (ITO) coated glass slide. Here, we compared the photoelectrochemical performance of a bare ITO electrode and a SnO_2 coated ITO electrode. As shown in Fig. 3, the fast rise photocurrent (Fig. 3d) is indicative of the efficient charge separation on the surface of the SnO_2 coated ITO electrode in $Ru(bpy)_2dppz^{2+}$ solution. Further study indicated that the produced anodic current showed good stability as well as quick response to 470 nm wavelength excitation (Fig. S1, ESI†). Thus, SnO_2 coated ITO electrode was selected as the working electrode.

The dependence of photocurrent on the applied bias potential is depicted in Fig. S2 (ESI†). The photocurrent increases upon biasing the potential in the region of −0.2 to +0.5 V in 9.0×10^{-8} M $Ru(bpy)_2dppz^{2+}$ solution. This can be explained that on the basis of the energetics and electron-transfer pathways involved in the anodic photocurrent

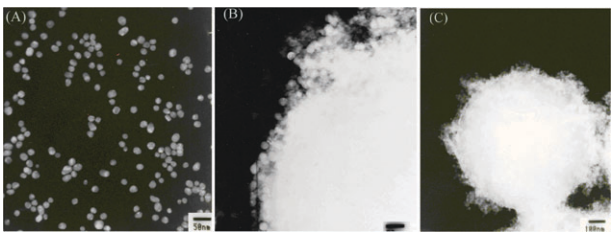

Fig. 1 TEM images of (A) AuNPs, (B) MB-bio-barcode conjugates and (C) MBs.

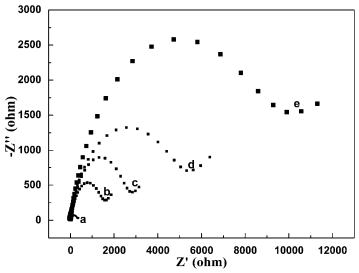

Fig. 2 Electrochemical impedance spectroscopy of different electrodes (a) the bare ITO electrode; (b) ITO/SnO_2; (c) ITO/SnO_2/APS; (d) ITO/SnO_2/APS/glutaraldehyde/aptamer; (e) ITO/SnO_2/APS/ glutaraldehyde/aptamer/biobarcode. Supporting electrolyte: 0.1 M pH 7.4 PBS containing 10 mM $Fe(CN_6)^{3-/4-}$ and 0.1 M KCl. The frequency range is between 1 and 100 kHz with an applied voltage of 10 mV.

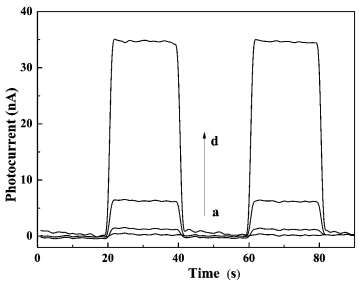

Fig. 3 The photocurrent response of (a) bare ITO electrode; (b) bare ITO electrode with 9×10^{-8} M $Ru(bpy)_2dppz^{2+}$; (c) ITO/SnO_2 electrode; (d) ITO/SnO_2 electrode with 9×10^{-8} M $Ru(bpy)_2dppz^{2+}$. Measurement was carried out in 10 mM Tris-HCl (pH = 7.0) containing 30 mM sodium oxalate. The excitation light was 470 nm and the light was turned on and off every 20 s. The applied potential was 0.1 V.

generation, a positive bias applied on the electrode will induce a higher photocurrent, whereas a negative bias will do the opposite.[20] Taking into account the blank value in 10 mM Tris-HCl buffer, a bias voltage of +0.1 V was selected in the following test.

The introduction of ATP at different concentrations induced different amounts of $Ru(bpy)_2dppz^{2+}$ immobilized on the electrode, which led to different photocurrent signals. A series of samples of ATP were determined by the present protocol, and the photocurrent peak height was utilized to evaluate the photoelectrochemical response to ATP. As shown in Fig. 4, as the concentration of ATP increased, the photocurrent signals were enhanced. A linear range from 1.0×10^{-8} to 1.0×10^{-6} M was observed with $\Delta I = 0.2188 + 3.625C_{ATP}$ (10^{-8} M) ($n = 12$, $R = 0.9993$) and a detection limit of 3.2×10^{-9} M was obtained. With the amplification by the bio-barcode method, the sensitivity of the proposed method is enhanced about 60-fold compared to a simple competitive process (Fig. S3 and S4, ESI†).

To assess the specificity of the developed method for the detection of ATP, aqueous solutions containing 4×10^{-7} M ATP, GTP (guanosine triphosphate), UTP (uridine triphosphate) and CTP (cytosine triphosphate) were tested under the same experimental conditions, respectively. As shown from Fig. 5, GTP, UTP or CTP did not induce any significant photocurrent signal as compared to that of ATP. This result agrees with the fact that the aptamer is specific

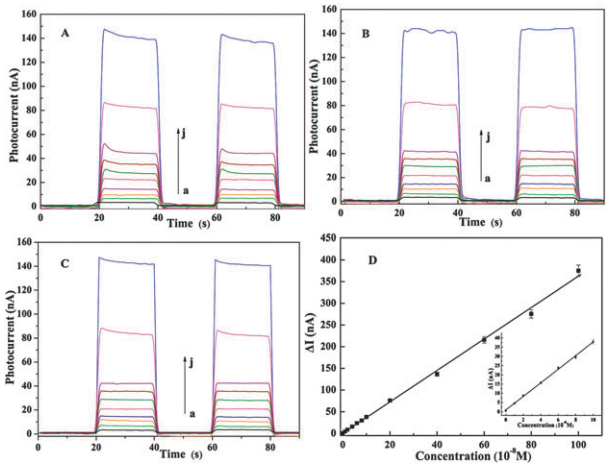

Fig. 4 (A)–(C) Three independent measurements for (a) ITO/SnO_2/APS/ glutaraldehyde/aptamer electrode in oxalate buffer. (b)–(j) Photocurrent responses of biosensor assembled as Scheme 1 with increasing levels of ATP (b) 0, (c) 1×10^{-8} M, (d) 2×10^{-8} M, (e) 4×10^{-8} M, (f) 6×10^{-8} M, (g) 8×10^{-8} M, (h) 1×10^{-7} M, (i) 2×10^{-7} M, (j) 4×10^{-7} M. (B) The calibration plot of peak current *vs.* the concentration of ATP from 1×10^{-8} to 1×10^{-6} M. Inset is the amplification of the linear range from 1×10^{-8} to 1×10^{-7} M for ATP determination. Measurement was carried out in 10 mM Tris-HCl (pH = 7.0) containing 30 mM sodium oxalate. The excitation light was 470 nm. The applied potential was 0.1 V.

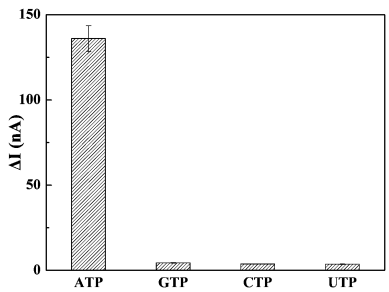

Fig. 5 Selectivity of ATP toward different analytes. The concentration of ATP, GTP, UTP and CTP was 4.0×10^{-7} M.

toward ATP, and may become a general method for any aptamer of interest.

In order to test the biological application of the proposed method, the ATP content in K562 leukemia cells was investigated. After diluting 100 fold, ATP extracts from K562 cells were subjected to photoelectrochemical detection. For comparison, the HPLC method was also used in determining the samples (see ESI†). The results of Table 1 showed that the concentration of ATP in K562 cell lysate was 3.43×10^{-6} M (average ± S.D., $n = 3$) per 10^5 cells, which was in good agreement with that obtained using the HPLC method.

Table 1 Analysis of ATP in K562 extracts

Sample[a]	This method/μM	RSD (%, $n = 3$)	HPLC/μM	RSD (%, $n = 3$)
1	3.48	4.5	3.75	2.0
2	3.29	3.2	3.61	3.1
3	3.51	3.8	3.52	2.6

[a] Each value is the average of three measurements for 10^5/mL K562 cells.

This result demonstrated that the developed strategy could be used to monitor the content of ATP in cell extracts exactly without the interference of other substance in cell.

In summary, the specificity of bio-barcoding and the recognition of aptamer have been integrated in photoelectrochemistry for the first time. The developed photoelectrochemical sensor was used in the detection of ATP and under the optimal conditions, a detection limit of 3.2×10^{-9} M was achieved. With its simplicity, selectivity, sensitivity and practicality in cell extract assay, this strategy shows great promise in the photoelectrochemical detection not only for the ATP, but also for other bio-active molecules. This can expand the application scope of photoelectrochemistry and be used as a powerful tool in molecule recognition.

This research was supported by National Natural Science Foundation (Nos.: 20905040, 20827005) and the National Basic Research Program of China (2010CB732404).

Notes and references

1 S. P. Song, Z. Q. Liang, J. Zhang, L. H. Wang, G. X. Li and C. H. Fan, *Angew. Chem., Int. Ed.*, 2009, **48**, 8670–8674.
2 S. Bi, H. Zhou and S. S. Zhang, *Chem. Commun.*, 2009, 5567–5569.
3 (*a*) X. B. Yin, Y. Y. Xin and Y. Zhao, *Anal. Chem.*, 2009, **81**, 9299–9305; (*b*) L. Z. Hu, Z. Bian, H. J. Li, S. Han, Y. L. Yuan, L. X. Gao and G. B. Xu, *Anal. Chem.*, 2009, **81**, 9807–9811.
4 (*a*) H. Yamada, K. Tanabe and S. Nishimoto, *Org. Biomol. Chem.*, 2008, **6**, 272–277; (*b*) T. V. Ran, Y. Omer, H. B. Yildiz, O. I. Wilner and I. Willner, *Angew. Chem., Int. Ed.*, 2008, **47**, 8272–8276; (*c*) Z. Q. Gao and N. C. Tansil, *Nucleic Acids Res.*, 2005, **33**, e123.
5 (*a*) M. M. Liang and L. H. Guo, *Environ. Sci. Technol.*, 2007, **41**, 658–664; (*b*) M. M. Liang, S. P. Jia, S. C. Zhu and L. H. Guo, *Environ. Sci. Technol.*, 2008, **42**, 635–639.
6 (*a*) S. L. Liu, C. Li, J. Cheng and Y. X. Zhou, *Anal. Chem.*, 2006, **78**, 4722–4726; (*b*) I. Willner, F. Patolsky and J. Wasserman, *Angew. Chem., Int. Ed.*, 2001, **40**, 1861–1864.
7 (*a*) N. Haddour, J. Chauvin, C. Gondran and S. Cosnier, *J. Am. Chem. Soc.*, 2006, **128**, 9693–9698; (*b*) G. L. Wang, P. P. Yu, J. J. Xu and H. Y. Chen, *J. Phys. Chem. C*, 2009, **113**, 11142–11148; (*c*) H. B. Yildiz, R. Freeman, R. Gill and I. Willner, *Anal. Chem.*, 2008, **80**, 2811–2816.
8 (*a*) J. A. Cooper, M. Wu and R. G. Compton, *Anal. Chem.*, 1998, **70**, 2922–2927; (*b*) V. Pardo-Yissar, E. Katz, J. Wasserman and I. Willner, *J. Am. Chem. Soc.*, 2003, **125**, 622–623.
9 L. M. Verstraeten, K. D. Coninck, K. Vlassak, W. Verstraete, H. Werf and M. Ilaiwi, *Soil Biol. Biochem.*, 1983, **15**, 397–402.
10 A. Lundin, M. Hasenson, J. Persson and A. Pousette, *Methods Enzymol.*, 1986, **133**, 27–42.
11 D. E. Huizenga and J. W. Szostak, *Biochemistry*, 1995, **34**, 656–665.
12 (*a*) Z. C. Xu, N. J. Singh, J. Lim, J. Pan, H. N. Kim, S. Park, K. S. Kim and J. Y. Yoon, *J. Am. Chem. Soc.*, 2009, **131**, 15528–15533; (*b*) Z. W. Tang, P. Mallikaratchy, R. H. Yang, Y. M. Kim, Z. Zhu, H. Wang and W. H. Tan, *J. Am. Chem. Soc.*, 2008, **130**, 11268–11269; (*c*) R. Nutiu and Y. Li, *J. Am. Chem. Soc.*, 2003, **125**, 4771–4778.
13 (*a*) X. Zuo, Y. Xiao and K. W. Plaxco, *J. Am. Chem. Soc.*, 2009, **131**, 6944–6945; (*b*) X. Zuo, S. Song, J. Zhang, D. Pan, L. Wang and C. Fan, *J. Am. Chem. Soc.*, 2007, **129**, 1042–1043.
14 J. Wang, L. Wang, X. Liu, Z. Liang, S. Song, W. Li, G. Li and C. Fan, *Adv. Mater.*, 2007, **19**, 3943–3946.
15 S. S. Zhang, Y. M. Yan and S. Bi, *Anal. Chem.*, 2009, **81**, 8695–8701.
16 W. Yao, L. Wang, H. Y. Wang, X. L. Zhang and L. Li, *Biosens. Bioelectron.*, 2009, **24**, 3269–3274.
17 J. Nam, S. I. Stoeva and C. A. Mirkin, *J. Am. Chem. Soc.*, 2004, **126**, 5932–5933.
18 S. Nakade, T. Kanzaki, W. Kubo, T. Kitamura, Y. Wada and S. Yanagida, *J. Phys. Chem. B*, 2005, **109**, 3480–3487.
19 G. L. Wang, J. J. Xu and H. Y. Chen, *Biosens. Bioelectron.*, 2009, **24**, 2494–2498.
20 K. Jiang, H. Xie and W. Zhan, *Langmuir*, 2009, **25**, 11129–11136.